Journal of Materials Chemistry C

Advances in Electro-copolymerization of NIR Emitting and Electronically Conducting Block Copolymers

Journal:	*Journal of Materials Chemistry C*
Manuscript ID	TC-COM-12-2018-006331.R2
Article Type:	Communication
Date Submitted by the Author:	20-Feb-2019
Complete List of Authors:	Rajapakse, R. M.; University of Peradeniya Postgraduate Institute of Agriculture; University of Mississippi, Chemistry & Biochemistry Attanayake, Nuwan ; Temple University, Chemistry Karunathilaka, Dilan ; University of Mississippi, Chemistry & Biochemistry Steen, April; University of Mississippi, Chemistry and Biochemistry Hammer, Nathan; University of Mississippi, Chemistry & Biochemistry Strongin, Daniel; Temple University, Chemistry Watkins, Davita; University of Mississippi, Chemistry & Biochemistry

Journal Name

COMMUNICATION

Advances in Electro-copolymerization of NIR Emitting and Electronically Conducting Block Copolymers

Received 00th January 20xx,
Accepted 00th January 20xx

DOI: 10.1039/x0xx00000x

www.rsc.org/

R. M. Gamini Rajapakse,[a]† Nuwan H. Attanayake,[b] Dilan Karunathilaka, [a] April E. Steen,[a] Nathan I. Hammer,[a] Daniel R. Strongin[b] and Davita L. Watkins [a] *

Block copolymers comprised of benzothiadiazole were successfully electro-copolymerized leading to $(BTD\text{-}T_2)_n(BTD\text{-}F_2)_m$, where *n* and *m* were varied in a perfectly controllable, well-defined manner. The polymers were characterized by cyclic voltammetry, AC-impedance, SEM-EDAX and XPS analyses. They exhibit absorbance and emission in the near infrared (NIR) region. Results support an efficient strategy towards the creation of even more complex materials with innumerable possible applications in opto-electronics.

Low-cost and straightforward synthesis of complex organic materials possessing unique electrical and optical properties have attracted world-wide attention for the development of novel electronic, optical, and opto-electronic devices. Since the discovery of electronically conducting polymers, the area of electropolymerization has developed exponentially, crossing borders of all facets of scientific disciplines.[1-4]

In contrast to chemical synthesis, electrosynthesis offers such opportunities since it is based on the addition or removal of electrons from electrical supplies, making it essentially reagent-free synthetic methodology.[5] As such, electrosynthesis is perhaps the cleanest and greenest way of synthesizing tailor-made organic compounds for desired applications.

Acknowledging these advantages, we have adopted electrosynthesis as a versatile technology towards tailor-made materials having unique electrical and optical properties. Herein, we reveal the electro-copolymerization of 4,7-dithiophen-2-yl-2,1,3-benzothiadiazole ($BTDT_2$) and 4,7-difuran-2-yl-2,1,3-benzothiadiazole ($BTDF_2$) leading to alternating and block copolymers (Fig. 1) with intriguing electronic and optical properties. We note that benzothiadiazole (BTD) based polymers of similar nature have been reported,[6-9] but never by means of electro-copolymerization in such a well-controlled and easily detectable fashion.

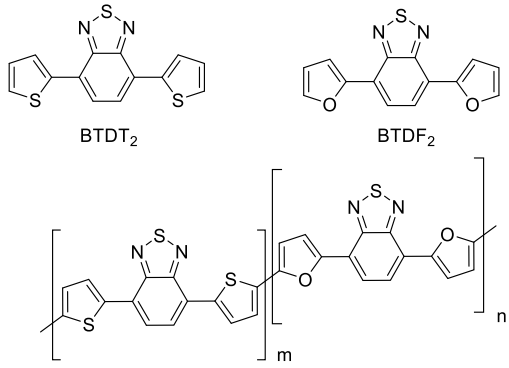

Figure 1. Structures of $BTDT_2$, $BTDF_2$ and $(BTDT_2)_m(BTDF_2)_n$ where m and n are 0:1, 1:0, 1:1 and 2:5.

Details of the electro-copolymerization for $BTDT_2$ and $BTDF_2$ taken in desired millimolar ratio of *m*:*n* are given in the Supporting Information (SI). The co-polymerization was achieved by repetitive 5 or 10 cyclic voltammetric (CV) experiments from + 0 V to 0.8 V or + 1.0 V or + 1.2 V depending on the $BTDF_2$ to $BTDT_2$ molar ratio; lower upper limit was taken when $BTDF_2$ amount is higher than $BTDT_2$ since furan is known to be unstable at high positive potentials.[10] The upper limit was chosen based on the amount of polymer deposited on the electrode surface without over oxidation of the polymer. Under argon, CVs were run at a 100 mV s^{-1} scan rate except for when scan rate dependence of peak currents was studied (Fig.2). In the latter case, scan rates were doubled: n^{*2} where n ranged from 3 to 10. After the polymer deposition on the working electrode (WE), the electrodes were rinsed with acetone and the CVs were run with background electrolyte (BGE) in the

[a] Department of Chemistry and Biochemistry, University of Mississippi, University, MS 38677-1848, USA. *Email - dwatkins@olemiss.edu
[b] Department of Chemistry, Temple University, 1901 North 13th Street, Philadelphia, Pennsylvania 19122, USA.
† RMGR is a visiting scholar at the University of Mississippi and is on leave from the University of Peradeniya, Sri Lanka; rmgr@pdn.ac.lk
Electronic Supplementary Information (ESI) available: [details of any supplementary information available should be included here]. See DOI: 10.1039/x0xx00000x

potential range between +1.2 V and -1.5 V (wrt SCE). Films were grown on FTO glass and rinsed with distilled water

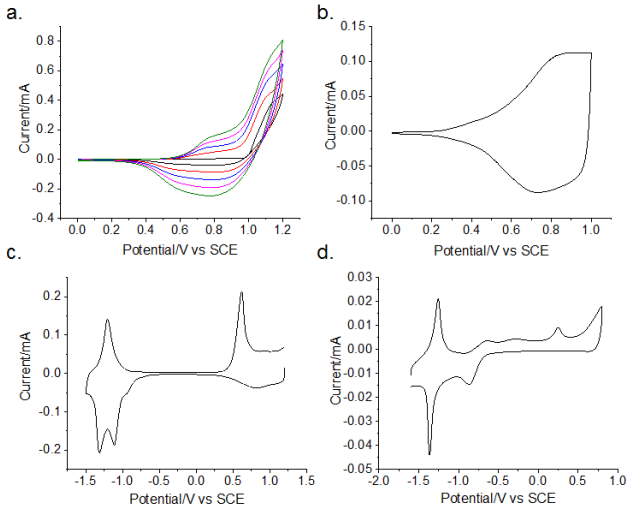

Figure 2. Repetitive CVs for the electropolymerization of $BTDT_2$ and $BTDF_2$ in 1:1 mol ratio (2.5 mmolar each) (a); CVs of the polymer from (b) 0 V to + 1.2 V at 100 mV $^{s-1}$ scan rate; (c) + 1.2 V to – 1.5 V for 1:1; and (d) + 1.2 V to – 1.5 V for 2:5 copolymer

and air dried for optical, microscopic and surface analytical studies. UV-visible spectra were recorded on polymer coated FTO glasses using bare FTO plates as reference. Small amounts of polymer samples were scraped off FTO surfaces for solid-state luminescence studies. Further details on experimental procedures are given in the SI.

The five CVs illustrating the electropolymerization of 1:1 molar ratios $BTDT_2$ to $BTDF_2$ are shown in Figure 2a. Similar CVs were obtained for other ratios (i.e., 2:5) and are given in the SI. The deposition of electronically conducting polymer film on WE surface is evident from the growth of currents in successive CVs. The CV of the polymer-coated WE made using 1:1 molar ratio of $BTDT_2$ and $BTDF_2$, run in the BGE, obtained in the positive direction from 0 V to + 1.2 V, is shown in Figure 2b. On the forward scan, the growth of current from ~0.16 V onwards followed by a plateau indicates the polymer film is gradually charging positively generating charge carriers such as polarons (extended conjugation of cation radicals) and bipolarons (extended conjugation of dications formed by the annihilation of free radicals forming a double bond when two polarons are combined).[11] It is possible that thiophene or furan units are accommodating these cation radicals and dications. These charge carriers are trapped within the polymer molecules thus giving them p-type character and associated electronic conductivity. The electrical neutralization is achieved by the ingress of counter ions (PF_6^-) ions.[12] On reversal, decline of the current to an essentially constant value indicates slow discharge of trapped charge carriers due to the injection of electrons. This discharing process continues towards high negative potentials up to -1.0 V where both copolymers show a typical reduction wave indicative of the neutralization of positively charged polymer backbones. Under these conditions, the polymers behave as insulators. When the potential is further scanned to higher negative values, more electrons are injected to the polymer generating anion radicals and dianions accommodated by BTD units such as BTD.- and -$BTDT_2(F_2)$BTD- species which can be considered as negatively charged polarons and bipolarons. It is interesting to note that trapped charges generated in the positive potentials remain in the polymers up to a very high negative potentials and this feature is demonstrated by the non-zero currents obtained in CVs in a wide range of potentials. When the potential is scanned back in the positive direction the trapped negative charge carriers slowly discharge up to about +0.6 V where the polymer becomes neutral and beyond these potentials it again acts as a p-type material.[13,14] This feature was evident in both homopolymers and copolymers synthesized. Additional data illustrating the electrochemical activity of the polymer grown with 1:1 and 2:5 molar ratios in both positive (p-type semiconducting), neutral (insulating) and negative (n-type semiconducting) potential domains are shown in Figure 2c and d, respectively.

Confirmation of both $BTDT_2$ and $BTDF_2$ in each copolymer was achieved by comparing reduction peaks positions relative to the two respective homopolymers. In contrast to the homopolymers where only one corresponding reduction peak is observed in -1.0 V to -1.5 V region (SI), the copolymers at all compositions show two reduction peaks. The two reduction peaks appearing in this potential region are due to the reduction of the BTD units in the polymers, thus making conjugated anion radicals (negative polarons). The $BTDT_2$ reduction appears first and can be assigned to the peak at -1.09 V while the peak appearing at a more negative potential of -1.35 V is due to reduction of $BTDF_2$ units of the copolymer synthesized using 1:1 molar ratio of the two monomers (Fig. 2c). The current values and calculated charge values obtained for the two peaks are equal in the 1:1 polymer, confirming that the polymer has a 1:1 ratio of $BTDT_2$ to $BTDF_2$ units in the polymer backbone. In addition, both reduction peaks are shifted towards less negative potentials relative to their homopolymers indicating that the BTD units in $BTDT_2$ and $BTDF_2$ are interacting with each other in 1:1 alternating fashion. In the polymer formed by taking 2:5 molar ratio, the current ratio of the two reduction peaks is 2:5 (Fig. 2d).

The reduction of the BTD unit in the polymer in the n-type region is determined by the diffusion-controlled ingress of counter ions as revealed by a linear relationship in the plot of peak current versus square root of scan rate for a peak at -1.32 V in the 1:1 alternating block copolymer (Fig. 3a). It can be concluded that the ratios of $BTDT_2$ and $BTDF_2$ in the copolymers is determined simply by the molar ratio of the monomers used in electropolymerization. As such, *m*:*n* block-copolymers of $BTDT_2$ and $BTDF_2$ can be grown via electropolymerization by taking appropriate molar ratios of the two monomers. Such control of block copolymers is not easy to obtain in chemical polymerization.

AC impedance analysis was achieved at different applied DC potentials to evaluate resistance values for electron transport along the polymer backbones (R_e). The ion transport between

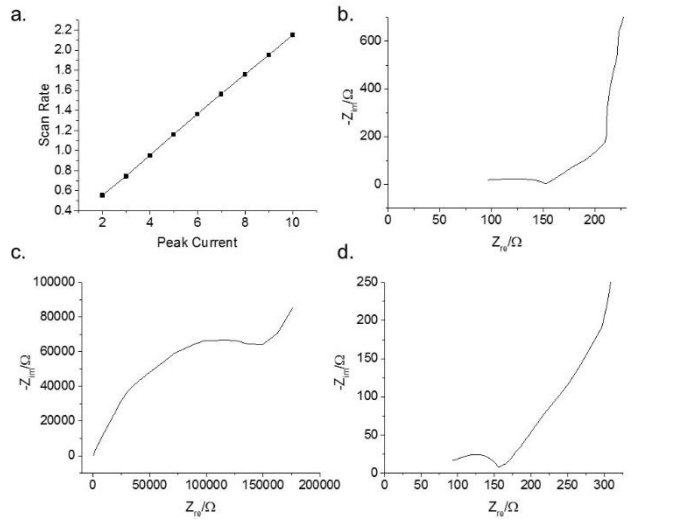

Figure 3. Plot of peak current versus square root of scan rate for the reduction peak at-1.35 V for 1:1 alternating polymer (a). Nyquist plots for AC impedance analysis of $BTDT_2$-$BTDF_2$ 1:1 alternating copolymer at +0.90 V (b), -0.80 V (c) and -1.22 V (d).

the solution and the polymer (R_I) to compensate charge on the polymer was also calculated. Nyquist [-Img(Z) vs Real(Z)] plots obtained at +0.90 V, -0.80 V and + 1.22 V DC applied potentials for 1:1 alternative block co-polymer are given in Figure 3, with additional plots in the SI. The dual rail transmission line model was used in analysing the Nyquist plots.[2, 15, 16] The Nyquist plots were interpreted using the equivalent circuit given in the SI which is the simplified version of the dual rail transmission line model proposed by Abery et al.[16, 17] The equivalent circuit is composed of serially connected electrical elements, R_s representing the series resistance, the circuit comprising of R_e the electron transport resistance connected in parallel with the double layer capacitance C_d, the Warberg impedance W, and lowest frequency capacitance, C. of the pure capacitive region of the polymer. All the Nyquist plots obtained experimentally were fitted to this equivalent circuit and simulated until the theoretical plot matches with the experimental one to less than 1% error. This simulation gives R_s, R_e, C_d, W and C values. The R_e thus obtained represents the resistance for electron transport along the polymer backbone. Note that the lower the R_e, the lower the resistance for electron transport and hence higher the electronic conductivity of the polymer. The dual rail transmission line model also gives coth functions which can be simplified to get the resistance, R_I, for ion ingress/egress to compensate charge of the polymer backbone. Detailed analysis shows that RI can be obtained by taking 1/3rd of the difference between the resistance obtained by extrapolating the lowest frequency, i.e., an almost vertical line to cut Z'-axis and the resistance obtained by extrapolating the Warberg impedance, i.e., straight line of 45˚ inclination, to cut Z'-axis. The R_e and R_I values are tabulated in Table S1. The dual rail transmission line circuit and simplified equivalent circuit model used to extract data are provide in the ESI.

Results conclude that all polymers are highly conducting at both positive (p-type) and negative (n-type) regimes but are insulators in the middle range between two conducting regimes.[17] Of interest to note is that R_e and R_I values are small and approximately equal—both the hole/electron transport along the polymer chain with concomitant ingress of counter ions for charge compensation are fast indicative of an excellent electronically conducting polymer in both n- and p-type potential domains. Interestingly, $BTDF_2$ becomes electroactive and conducting above +0.6 V up to +1.2 V, but $BTDT_2$ becomes so above +0.8 V. Both polymers have appreciable conductance in the negative potential regime below -1.0 V. The copolymers have acquired properties of both homopolymers and are electroactive and conducting above +0.6 V in the positive regime and below -1.0 V in the negative regime. R_e values obtained for copolymers are an order of magnitude lower than those of homopolymers (SI-Table 1). Copolymers also show electrical conductivity over wider potential ranges as well as increased current densities when compared to homopolymers. Notably, the resistance for ion transport at each potential for all polymers is lower than that for electron transport; usually the opposite is observed.[18] This may be due to the highly porous globular structure capable of accompanying solution pockets within the polymers to facilitate rapid ionic transport between the polymer backbone and accompanying electrolyte solution.

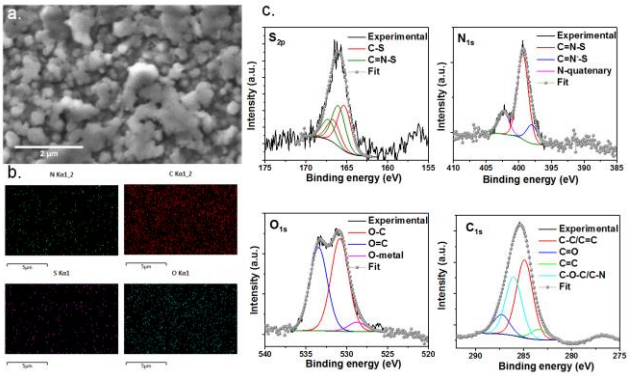

Figure 4. SEM image of $BTDT_2$-$BTDF_2$ 1:1 alternating copolymer, n-type (a); elemental mapping (b); and XPS fitting confirming atomic ratios (c).

The globular bulb like morphology is shown in the SEM image of 1:1 alternating copolymer deposited on FTO glass (Fig. 4a). The morphology is due to the lack of microscopic uniformity of the FTO plate. SEM image of bare FTO reveals grains of FTO which afford polymer growth in an epitaxial manner. The atomic ratios obtained from SEM-EDX are also complicated due to the interference from the atoms of FTO and glass substrate. When the polymer film thickness is increased (i.e., 500 nm to 600 nm), less FTO is exposed and elemental mapping at the macroscopic scale shows acceptable atomic levels of carbon, nitrogen, oxygen and sulfur that support copolymerization (Fig. 4b).

Data obtained by elemental mapping and XPS analyses are more conclusive; however, the counter ions (i.e, PF_6^- and Bu_4N^+ from BGE) present in solvent pockets of the polymer make the exact fitting of atom ratios difficult (Fig. 4b,c; Table S2). All the polymers contain varying amounts of quaternary ammonium ions coming from the BGE which increases the N-atomic

percentage. On average, the reduced (negative, n-type) form of the 1:1 alternating copolymer has more carbon than the oxidized (positive, p-type) form (~70 versus 50 carbon atomic %, respectively), again indicating the possession of higher quaternary ammonium ions in the n-type polymer as counter ions.

Figure 4c shows nitrogen and sulfur in different electronic environments with corresponding binding energies of the deconvoluted XPS peaks. In both p- and n-type alternating block copolymers, N=S=N (BTD), C-S-C (thiophene) and C-O-C (furan) peaks are present. With respect to those of the monomer, BTD nitrogen and deconvoluted sulfur peaks of BTD and thiophene can be identified with the latter appearing at a higher binding energy than those of the former two (Table S2). Comparing the homopolymers to that of the 1:1 alternating copolymer, sulfur peaks were resolved and fitted to BTD [N=S=N; 165.2 eV p-type; 165.0 eV n-type] and thiophene [C-S-C; 165.5 eV p-type; 166.0 eV n-type]. XPS analysis of oxygen further confirms copolymerization revealing two peaks: one belonging to furan [C-O-C; 533.4 eV p-type; 533.5 eV n-type] and the other to tin oxide from the FTO substrate (530.9 eV).[19, 20] Variation in binding energies attest to an effective polarization between the BTD and thiophene/furan units affording an ambipolar nature within the polymers which is more prominent in the copolymers than in homopolymers. Such can contribute to an increased number of electric charge carriers, leading to higher electrical conductivity for the copolymers as revealed by AC impedance studies. Note also that $BTDT_2$ homopolymer contains both sulfur peaks associated with BTD [N=S=N; 164.8 eV p-type; 166.0 eV n-type] and thiophene [C-S-C; 165.2 eV p-type; 166.4 eV n-type] as well as one O peak from FTO which appear at their exact binding energies (Fig. S6). $BTDF_2$ hompolymer contains only one sulfur peak corresponding to BTD [N=S=N; 165.7 eV p-type; 166.2 eV n-type] but two oxygen peaks corresponding to FTO and furan (Fig. S7). Both copolymers in each doping state contain two sulfur peaks and two oxygen peaks demonstrating that they have BTD, thiophene and furan. Attempts were made to quantify thiophene to furan ratio to confirm the formation of 1:1 and 2:5 molar ratios of $BTDT_2$ and $BTDF_2$ in the two copolymers. However, the task was rather challenging as the intensities of oxygen peaks are much higher than those of the other elements due to the presence of oxygen in the substrate FTO.

Nevertheless, XPS confirms the formation of copolymers. Elemental mapping diagrams show approximately 2:1 ratio in sulfur to oxygen in the mapped areas of the 1:1 copolymer (Table S2). This agrees with the theoretical atomic ratio of 4:2 in the $BTDT_2$-$BTDF_2$- repeat unit. Additional investigation of SEM/EDAX spectra for more direct quantitative results of polymer films with varying ratios of monomer are currently underway.

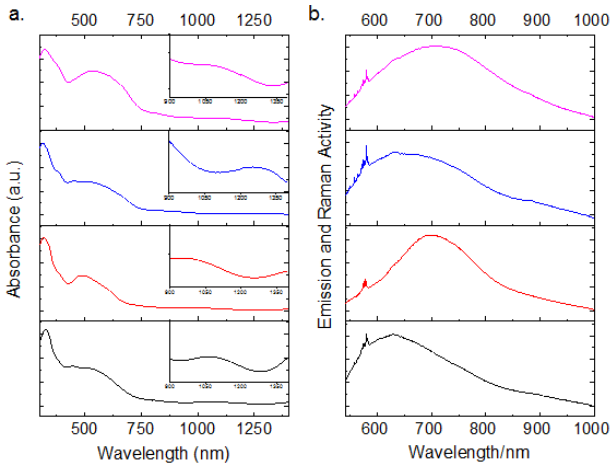

Figure 5. UV-visible-NIR absorption (a) and emission (b) spectra of $BTDT_2$ (black), $BTDF_2$ (red), and 1:1 block copolymer: p-type (blue) and n-type (purple).

UV-visible absorption spectra of the 1:1 alternating copolymer in its p-type and n-type conducting states are shown in Figure 5. Those of the homopolymers are also given in Figure 5; absorption spectra of copolymers have been included in the SI. The p-type polymer exhibits absorption up to 700 nm and those of the n-type polymer extend up to 1000 nm. When the polymers are n-doped the electron density of the polymer backbone increases affording band gaps as low as 1.24 eV. The 1:1 alternating copolymer in its p-type state has a band gap of 1.65 eV and that of 1.59 eV for its n-type state. Both possesses additional absorbance bands between 1080-1300 nm. Fluorescence spectra indicate emission in the NIR region with broad bands extending into the NIRII window. The 1:1 alternating copolymer in its p-type state has emission λ_{max} of 657 nm and that of 710 nm for its n-type state. The broadened absorbance and emission bands are presumably due to overlapping of maxima of the two monomer components further supporting that the alternating copolymer has a 1:1 ratio of $BTDT_2$ to $BTDF_2$. Despite variations in optical properties, the Raman spectra of n- and p-type are identical (Fig. S8) as the molecular frameworks and vibrational frequencies of the two polymers are relatively the same.

In conclusion, a low-cost and straightforward synthetic strategy towards complex organic conjugated polymers with perfectly controlled stoichiometric ratios has been presented. Our goal is to be able to study additional molar ratios and apply the technique to more difficult substrates for the tailoring of next generation opto-electronic materials.

Conflicts of interest

There are no conflicts to declare.

Acknowledgment

R.M.G.R, D.K. and D.L.W. appreciate financial support of this work from the National Science Foundation CAREER Award under Grant

Numbers CHE-1652094. A.E.S. and N.I.H. acknowledge support from the National Science Foundation Grant Number OIA-1539035 and CHE-1532079. N.H.A and D.R.S. acknowledges support from the Center for Complex Materials from First Principles, an Energy Frontier Research Center funded by the U.S. Department of Energy, Office of Science, Basic Energy Sciences under Award # DE-SC001257.

Notes and references

1. M. R. J. Scherer, in *Double-Gyroid-Structured Functional Materials: Synthesis and Applications*, Springer International Publishing, Heidelberg, 2013, DOI: 10.1007/978-3-319-00354-2_7, pp. 135-156.
2. J. Heinze, Berlin, Heidelberg, 1990.
3. S. C. Rasmussen, in *100+ Years of Plastics. <break></break>Leo Baekeland and Beyond*, American Chemical Society, 2011, vol. 1080, ch. 10, pp. 147-163.
4. D. J. Walton, *Materials & Design*, 1990, **11**, 142-152.
5. J. Heinze, B. A. Frontana-Uribe and S. Ludwigs, *Chemical Reviews*, 2010, **110**, 4724-4771.
6. K. Kawabata, M. Takeguchi and H. Goto, *Macromolecules*, 2013, **46**, 2078-2091.
7. C. Kitamura, S. Tanaka and Y. Yamashita, *Chemistry of Materials*, 1996, **8**, 570-578.
8. A. A. Tsegaye, T. T. Waryo, P. G. Baker and E. I. Iwuoha, *Materials Chemistry and Physics*, 2016, **171**, 57-62.
9. E. Bundgaard and F. C. Krebs, *Macromolecules*, 2006, **39**, 2823-2831.
10. D. Sheberla, S. Patra, Y. H. Wijsboom, S. Sharma, Y. Sheynin, A.-E. Haj-Yahia, A. H. Barak, O. Gidron and M. Bendikov, *Chemical science*, 2015, **6**, 360-371.
11. D. Fichou, G. Horowitz, B. Xu and F. Garnier, *Synthetic Metals*, 1990, **39**, 243-259.
12. I. Shown, A. Ganguly, L.-C. Chen and K.-H. Chen, *Energy Science & Engineering*, 2015, **3**, 2-26.
13. A. R. Hillman and E. F. Mallen, *Electrochimica Acta*, 1992, **37**, 1887-1896.
14. A. R. Hillman and E. F. Mallen, *Journal of the Chemical Society, Faraday Transactions*, 1991, **87**, 2209-2217.
15. W. J. Albery and A. R. Mount, *Journal of the Chemical Society, Faraday Transactions*, 1994, **90**, 1115-1119.
16. W. J. Albery and A. R. Mount, in *Electroactive Polymer Electrochemistry: Part 1: Fundamentals*, ed. M. E. G. Lyons, Springer US, Boston, MA, 1994, DOI: 10.1007/978-1-4757-5070-6_4, pp. 443-483.
17. A. G. MacDiarmid and A. J. Epstein, *MRS Proceedings*, 2011, **328**, 133.
18. J. F. Rubinson and Y. P. Kayinamura, *Chemical Society Reviews*, 2009, **38**, 3339-3347.
19. D. K. Bora, *Materials Science in Semiconductor Processing*, 2015, **31**, 728-738.
20. M. G. Olayo, R. Zúñiga, F. González-Salgado, L. M. Gómez, M. González-Torres, R. Basurto and G. J. Cruz, *Polymer Bulletin*, 2017, **74**, 571-581.

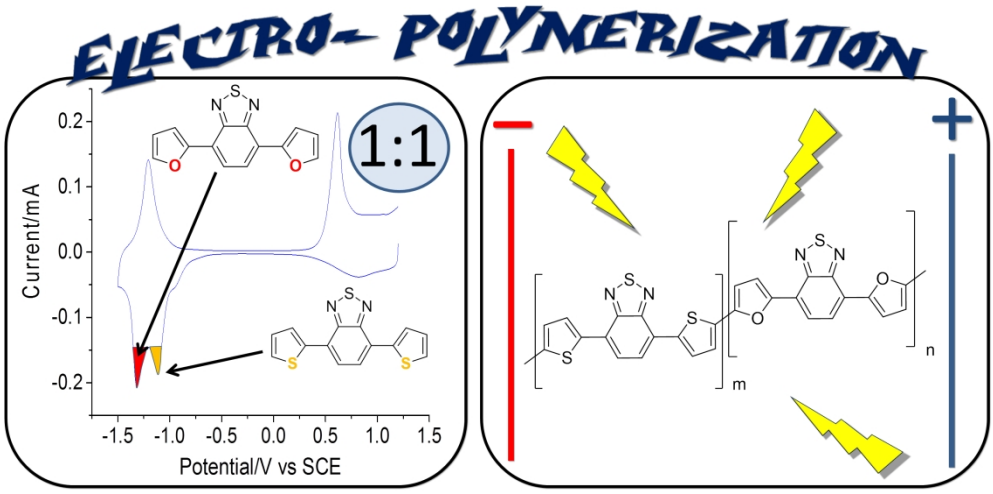

1219x609mm (64 x 64 DPI)